The Canadian Mineralogist
Vol. 32, pp. 873-884 (1994)

CHARACTERIZATION OF THE $FeSO_4 \cdot H_2O$ – $CuSO_4 \cdot H_2O$ SOLID-SOLUTION SERIES, AND THE NATURE OF POITEVINITE, $(Cu,Fe)SO_4 \cdot H_2O$

GERALD GIESTER AND CHRISTIAN L. LENGAUER

Institut für Mineralogie und Kristallographie, Universität Wien, Dr. Karl Lueger-Ring 1, A-1010 Vienna, Austria

GÜNTHER REDHAMMER

Institut für Mineralogie, Universität Salzburg, A-5020 Salzburg, Austria

ABSTRACT

Various members of the $FeSO_4 \cdot H_2O$ – $CuSO_4 \cdot H_2O$ kieserite-type solid-solution series were synthesized and investigated by X-ray powder diffraction and Mössbauer spectroscopy. Comparison of the Fe/Cu molar ratio between the precursor aqueous solutions and the products of precipitation revealed a preferred incorporation of Fe into the structure. End-member szomolnokite, $FeSO_4 \cdot H_2O$, is monoclinic, and synthetic $CuSO_4 \cdot H_2O$ is triclinic. The cell-parameter refinements of $(Fe,Cu)SO_4 \cdot H_2O$ compounds show a reduction in symmetry from monoclinic to triclinic beyond 20 mol.% Cu. By Mössbauer spectroscopy, significant ordering involving the cations can be observed only in members of the solid solution with more than 20 mol.% Cu. Site ordering is characterized by a preference of ferrous iron for the less distorted site. The similar scattering factors of Fe and Cu do not allow the cation distribution to be refined by X-ray methods. The structure of the investigated compounds with more than 20 mol.% Cu agrees with the triclinic model for $CuSO_4 \cdot H_2O$. Poitevinite is a distinct mineral species because of cation site-ordering and of the triclinic distortion of the structure. Its cell parameters, obtained by Rietveld refinement in space group $P\bar{1}$, are: a 5.120(1), b 5.160(1), c 7.535(2) Å, α 107.06(1), β 107.40(1), γ 92.73(1)°, and in space group $C\bar{1}$: a 7.094(1), b 7.440(1), c 7.824(2) Å, α 89.47(1), β 119.56(1), γ 90.45(1)°. The structural formula of poitevinite, as derived from ICP and Mössbauer data, is $[Cu_{0.28}(Fe,Zn)_{0.22}]\,[Cu_{0.19}(Fe,Zn)_{0.31}]SO_4 \cdot H_2O$.

Keywords: poitevinite, $(Cu,Fe)SO_4 \cdot H_2O$, kieserite group, Rietveld refinement, Mössbauer spectroscopy, triclinic distortion.

SOMMAIRE

Nous avons synthétisé et caractérisé divers membres de la solution solide de type kieserite [$FeSO_4 \cdot H_2O$ – $CuSO_4 \cdot H_2O$] par diffraction X (méthode des poudres) et par spectroscopie de Mössbauer. Une comparaison des rapports molaires Fe/Cu de la solution aqueuse de départ et des précipités révèle une incorporation préférentielle du Fe dans la structure. Le pôle szomolnokite, $FeSO_4 \cdot H_2O$, est monoclinique, tandis que le $CuSO_4 \cdot H_2O$ synthétique est triclinique. Les paramètres réticulaires de composés $(Fe,Cu)SO_4 \cdot H_2O$ révèlent une réduction dans la symétrie, de monoclinique à triclinique, à un seuil de 20% de Cu (base molaire). Les spectres de Mössbauer démontrent une mise en ordre importante uniquement dans les compositions dont la teneur en Cu dépasse 20%. Cette mise en ordre témoigne d'une préférence du Fe^{2+} pour le site le moins irrégulier. Le comportement très semblable du Fe et du Cu par rapport à la dispersion des rayons X ne permet pas un affinement de la distribution des cations dans le site occupé. La structure des composés contenant plus que 20% du pôle Cu concorde avec un modèle triclinique pour $CuSO_4 \cdot H_2O$. La poitevinite est considérée une espèce distincte à cause de la mise en ordre des cations dans ce même site, et la distorsion qui en résulte, menant à la symétrie triclinique. Ses paramètres réticulaires, affinés par méthode de Rietveld dans le groupe spatial $P\bar{1}$, sont a 5.120(1), b 5.160(1), c 7.535(2) Å, α 107.06(1), β 107.40(1), et γ 92.73(1)°, ou, dans le groupe spatial $C\bar{1}$, a 7.094(1), b 7.440(1), c 7.824(2) Å, α 89.47(1), β 119.56(1), et γ 90.45(1)°. La formule structurale de la poitevinite, d'après les données obtenues par plasma avec induction couplée (ICP) et par spectroscopie de Mössbauer, serait $[Cu_{0.28}(Fe,Zn)_{0.22}][Cu_{0.19}(Fe,Zn)_{0.31}]SO_4 \cdot H_2O$.

(Traduit par la Rédaction)

Mots-clés: poitevinite, $(Cu,Fe)SO_4 \cdot H_2O$, groupe de la kieserite, affinement de Rietveld, spectroscopie de Mössbauer, distorsion triclinique.

INTRODUCTION

Poitevinite was first described by Jambor (1962) and Jambor *et al.* (1964) from Bonaparte River, British Columbia; they proposed the formula $(Cu_{0.50}Fe_{0.46}Zn_{0.08})SO_4 \cdot 1.2H_2O$, which can be idealized as $(Cu,Fe)SO_4 \cdot H_2O$. From X-ray-diffraction data, they assigned it to the kieserite group (monoclinic). Oswald (1965), Coing-Boyat & Le Fur (1966) and Giester (1988) showed that the copper end-member of this group is triclinic. Therefore, one might infer that poitevinite shows a similar distortion of the structure. A reduction in symmetry from space group *C2/c* as in kieserite, $MgSO_4 \cdot H_2O$, to space group $P\bar{1}$ causes the M^{2+} position to be split into two positions ($M1^{2+}$, $M2^{2+}$). The copper atom, with its preference for distorted octahedral environment (owing to the Jahn–Teller effect), should occupy the more irregular $M^{2+}O_6$ polyhedron. The characteristic arrangement of the $M^{2+}O_6$ octahedra, linked via the $O(H_2O)$ atom to chains parallel [001] (kieserite setting), is illustrated in Figure 1. In a triclinic structure, the $M1^{2+}O_6$ and $M2^{2+}O_6$ polyhedra alternate. For reviews on kieserite-group compounds and related structures, the reader is referred to Baur (1959), Hawthorne *et al.* (1987), Giester (1988), Groat *et al.* (1990), Zemann (1990), Wildner & Giester (1991) and Giester & Wildner (1992).

EXPERIMENTAL

Syntheses

The pure compounds and ten mixtures of $CuSO_4 \cdot 5H_2O$ (Merck Product No. 2790) and $FeSO_4 \cdot 7H_2O$ (Merck Product No. 3965) in different molar ratios were dissolved in water and subsequently treated in three ways: (1) The solutions were heated to 380 K on a temperature-controlled stirring apparatus, and concentrated sulfuric acid (Merck Product No. 731) was added until rapid precipitation of the monohydrate compounds occurred. (2) The semicon-

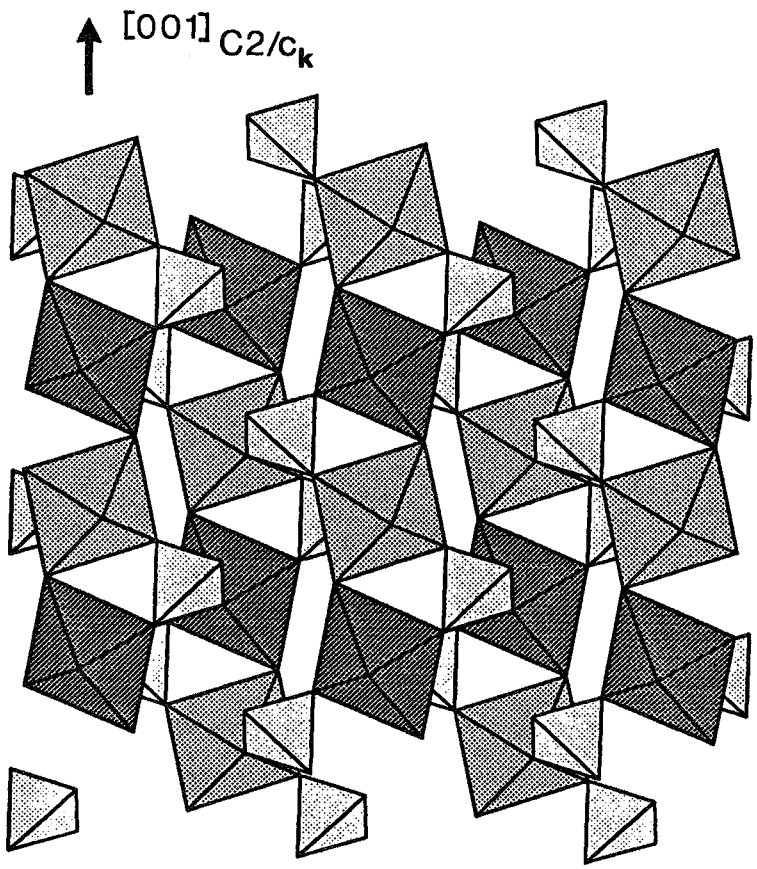

FIG. 1. Projection of the crystal structure of poitevinite showing the chains of *M*1 and *M*2 octahedra parallel to [111]. This direction, corresponding to [001] in the kieserite setting $C2/c_K$, is indicated by an arrow. The structure drawing was prepared with the program ATOMS (Dowty 1993).

TABLE 1. PREPARATION, CHEMICAL DATA, AND METHODS OF INVESTIGATIONS EMPLOYED TO CHARACTERIZE THE VARIOUS SAMPLES

Cu_{100}[1]	Cu_{100}[2]	-	-	RR[3]	-	(1)[4]
$Cu_{86}Fe_{14}$	$Cu_{80}Fe_{20}$	XRF[5]	ICP[5]	RR	Mö[6]	(1)
$Cu_{80}Fe_{20}$	$Cu_{74}Fe_{26}$	XRF	ICP	RR	Mö	(1)
$Cu_{75}Fe_{25}$	$Cu_{67}Fe_{33}$		ICP	RR		(3)
$Cu_{66}Fe_{34}$	$Cu_{55}Fe_{45}$	XRF	ICP	RR	Mö	(1)
$Cu_{66}Fe_{34}$	$Cu_{46}Fe_{54}$	XRF	ICP	RR	-	(3)
$Cu_{75}Fe_{25}$	$Cu_{41}Fe_{59}$	XRF	ICP	RR	-	(2)
$Cu_{66}Fe_{34}$	$Cu_{34}Fe_{66}$	XRF	ICP	RR	-	(2)
$Cu_{50}Fe_{50}$	$Cu_{29}Fe_{71}$	XRF	ICP	RR	-	(2)
$Cu_{50}Fe_{50}$	$Cu_{25}Fe_{75}$	XRF	ICP	RR	Mö	(1)
$Cu_{34}Fe_{66}$	$Cu_{19}Fe_{81}$	XRF	ICP	RR	-	(1)
Fe_{100}	Fe_{100}	-	-	RR	Mö	(1)
	$Cu_{48}Fe_{52}$	XRF	ICP	RR	Mö	poitevinite[7]

[1]molar Cu/Fe ratio in the precursor liquids, [2]molar Cu/Fe ratio in the precipitates, [3]Rietveld refinement, [4]methods of synthesis (see text), [5]type of chemical analysis, [6]Mössbauer spectroscopy, [7]Fe = Fe + Zn.

centrated solutions were evaporated slowly with minor amounts of H_2SO_4 at temperatures of 330 K under vacuum over a period of one week. (3) Solutions were evaporated at 1 atm. in a temperature-controlled sand bath at temperatures of 380 K. Details are compiled in Table 1.

In order to minimize the effects of the incongruent precipitation, *i.e.*, preferred incorporation of ferrous iron with respect to the bulk solution, the investigated samples were extracted at an initial stage of the crystallization process. Temperature and acidity are critical to avoid the coprecipitation of chalcocyanite or bonattite compounds. Depending on the method of synthesis, the monohydrate compounds form a microcrystalline powder (1) or radially intergrown aggregates of crystals with individual sizes up to some tenths of a millimeter (2, 3). In contrast to the nearly colorless end-members, the intermediate phases of the solid solution are reddish orange, with the most intense color occurring in the equimolar compound. This finding is consistent with the observation that poitevinite is salmon-colored.

The phases prepared by method (1) were subsequently treated for six hours at 380 K under reducing conditions (30 vol.% hydrogen, 70 vol.% nitrogen) to improve crystallinity and cation order.

Chemical analysis

The Cu:Fe ratio of poitevinite and the synthetic products was determined by X-ray-fluorescence analysis (XRF) using four external standards: mixtures of the end members and $B(OH)_3$ were pressed into a disk. The measurements were performed on a Philips PW1030 instrument, with Rh radiation. In addition, the samples were dissolved in $(HCl)_{conc.}$ and analyzed by inductively coupled plasma with atomic absorption spectroscopy (ICP–AAS) using an ARL–3520–ICP (Paschen–Runge) instrument. For the thermogravimetric investigation, a computer-controlled Mettler M3 microbalance combined with a TA4000 Thermo-Analysis System was used in the range 300–900 K under a nitrogen atmosphere, with a heating rate of 5 K/min.

X-ray powder diffraction

The X-ray measurements were done on a Philips PW3020 diffractometer equipped with automatic divergence slit, sample spinner, graphite secondary monochromator, scintillation counter using Cu$K\alpha$ radiation (45 kV, 35 mA). A receiving slit of 0.1 mm was used. Soller slits were used on the primary and secondary side. According to Bowden & Ryan (1991), an antiscatter slit of 4° 2θ was selected. The fine-grained powders were back-loaded into stainless-steel sample holders 15 mm in diameter. For poitevinite, the powder was fixed on a low-background silicon single-crystal using acetone. The measurements were done in step-scan mode over the range 5–135° 2θ in steps of 0.02° with a counting time of 5.0 s/step.

Rietveld refinement

The Rietveld refinements and the distance and angle calculations were done with the Philips "PC–Rietveld plus" package (Fischer *et al.* 1993). More sophisticated refinements were performed with the program RERIET (Kassner 1993). The recorded data were treated by a manual background-correction, as the contribution of the sample holder could not be fitted by a polynomial function. An automatic-to-fixed divergence-slit conversion was applied to the Lorentz-polarization factor in the first peak-simulation process during the refinement process (Fischer 1993). The pseudo-Voigt profile function was used for the simulation of the peak shape, with two parameters refining the Lorentzian part of the peaks as a function of 2θ. Owing to severe overlap of peaks, caused by the triclinic symmetry of the cell, intensities within only six times the full width at half maximum (FWHM) were considered to contribute to a reflection. Peaks below 25° 2θ were corrected for asymmetry effects after Rietveld (1969). The angular dependence of FWHM was refined with three parameters using the formula of Caglioti *et al.* (1958). Twenty-four structural and five profile parameters were refined. The X-ray-scattering factors for the cations in their respective valence state were taken from the International Tables for X-ray Crystallography (1974) and the values for O^{2-} are from Hovestreydt (1983).

In the case of scorodite impurities, a multiphase refinement was applied; we constrained the mixing parameters in the pseudo-Voigt function and the first and second term of the FWHM formula.

Mössbauer spectroscopy

Mössbauer spectra were recorded at 77 K and 293 K using a conventional Mössbauer spectrometer (source 50 mCi, ^{57}Co/Rh, a multichannel analyzer with 1024 channels, electromechanical drive system, symmetrical triangular movement). Spectra were recorded at the temperature of liquid nitrogen with the source at room temperature and the absorber at 77 K. The spectrometer velocity was calibrated against an α-Fe foil. The two symmetrical spectra obtained were folded and evaluated assuming Lorentzian line-shape. The linewidth of the two Fe^{2+} doublets was refined with one common parameter. The Mössbauer data were evaluated by the least-squares program MOESALZ (Forcher *et al.* 1992).

Poitevinite

The type material, obtained from the Royal Ontario Museum (No. M–25440), consists of a fine, salmon-colored powder with impurities of quartz, gypsum, pyrite, bonattite ($CuSO_4 \cdot 3H_2O$) and scorodite ($FeAsO_4 \cdot 2H_2O$). The impurities of scorodite (approximately 25 wt.% by Mössbauer spectroscopy) could not be eliminated entirely by hand picking. A multiphase Rietveld refinement reveals cell parameters of scorodite [*a* 8.932(2), *b* 10.299(3), *c* 10.037(2) Å], in good agreement with the data for synthetic $FeAsO_4 \cdot 2H_2O$ [*a* 8.90, *b* 10.33, *c* 10.05 Å: PDF 26–778]. Thus, incorporation of copper in the structure of scorodite is considered unlikely. The iron content in poitevinite was corrected accordingly.

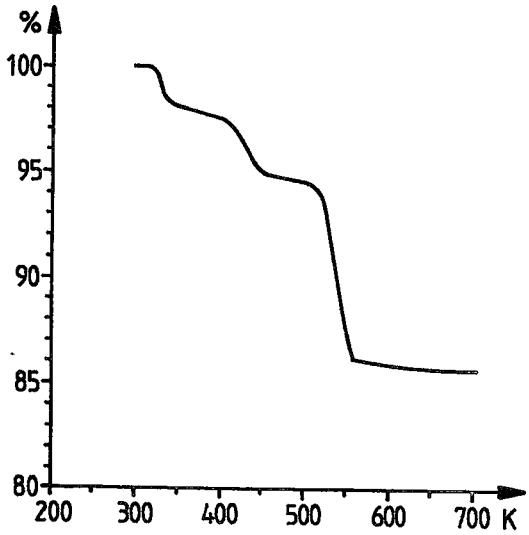

FIG. 2. Results of a thermogravimetric analysis of a sample of poitevinite (2.58 mg, 5 K/min).

A thermogravimetric analysis (Fig. 2) of the material as received reveals a loss of water in three steps. The maxima of the first derivative are at 330, 430 and 540 K, with approximate values of –2, –2 and –9 wt.%, respectively. The synthetic samples exhibit only the decomposition step at approximately 540 K. As scorodite contains two H_2O molecules in the formula unit, step 1 and 2 may be assigned to the impurity. The main loss of 9 wt.% fits approximately the ideal value of 10.4 wt.% H_2O in poitevinite. Jambor (1962) gave a water content of 12.07 wt.%; the high value reflects the scorodite impurity.

Chemical analysis of 8.7 mg of hand-picked poitevinite by ICP (Table 1) gives the formula $(Cu_{0.45}Fe_{0.49}Zn_{0.06})SO_4 \cdot H_2O$. Taking the scorodite contamination into account, the revised formula, $(Cu_{0.48}Fe_{0.45}Zn_{0.07})SO_4 \cdot H_2O$, is close to that proposed by Jambor *et al.* (1964). Because of their similar crystallochemical behavior, ferrous iron and zinc were treated as Fe^{2+} in our calculations.

X-RAY POWDER INVESTIGATION

Indexing

For purposes of indexing, the reduced triclinic setting given by Giester (1988) was used to describe the cell. For the description in the monoclinic system, the original setting of kieserite according to Leonhardt & Weiss (1957) in space group *C*2/*c* (hereafter denoted as $C2/c_K$) was chosen, in which the [001] axis is oriented parallel to the $M^{2+}O_6$ chains. Note that this setting of kieserite is not in accordance with the common practice of choosing unit axes. The original setting of kieserite can be transformed to a "reduced" monoclinic setting in *C*2/*c* by shifting the origin (owing to an additional *n*-glide plane in $y = \frac{1}{4}$), further denoted as $C2/c_R$. This gives rise to difficulties when comparing cell parameters and indexing of kieserite-type compounds (*cf.* Isaacs & Peacor 1981), especially with powder data. In addition, some kieserite-related structures like lacroixite, $NaAlPO_4 \cdot F$ (Lahti & Pajunen 1985) are distorted in such a way that the direction of the $M^{2+}O_6$ chains is shorter than the related diagonal in the (001) plane. The corresponding transformation-matrices between the particular settings are as follows. The matrix transformations were performed with the program CRYSCOMP (Bohm 1992):

$C2/c_K \rightarrow C2/c_R$ (100/0$\bar{1}$0/$\bar{1}$0$\bar{1}$)
$P\bar{1} \rightarrow C2/c_R$ ($\bar{1}\bar{1}$0/$\bar{1}$10/00$\bar{1}$)
$P\bar{1} \rightarrow C2/c_K$ (110/1$\bar{1}$0/$\bar{1}\bar{1}\bar{1}$)

Cell-parameter refinement

A general view of the variation of the cell parameters by Rietveld refinement (Table 2) is clearly rep-

TABLE 2. OBSERVED CELL PARAMETERS FROM RIETVELD REFINEMENT AND LITERATURE DATA ON $(Fe,Cu)SO_4 \cdot H_2O$ COMPOUNDS AND POITEVINITE

	reduced triclinic setting ($P\bar{1}$)							kieserite setting ($C2/c_R$)							
	a	*b*	*c*	*α*	*β*	*γ*	*V*	*a*	*b*	*c*	*α*	*β*	*γ*	*V*	Ref.
Cu_{100}	5.037(1)	5.170(1)	7.578(2)	108.62(1)	108.39(1)	90.93(1)	175.95	7.159	7.276	7.719	89.09	118.90	91.49	351.91	(2)
Cu_{100}	5.038(9)	5.170(9)	7.575(9)	108.6(1)	108.4(1)	90.9(1)	176.01	7.162	7.275	7.722	89.08	118.92	91.48	352.03	(4)
Cu_{100}	5.034(1)	5.167(1)	7.573(2)	108.64(1)	108.41(1)	90.88(1)	175.61	7.158	7.269	7.713	89.09	118.91	91.49	351.21	(1)
$Cu_{80}Fe_{20}$	5.061(1)	5.167(1)	7.558(2)	107.75(1)	108.13(1)	91.76(1)	177.16	7.121	7.343	7.760	88.91	119.13	91.19	354.32	(1)
$Cu_{74}Fe_{26}$	5.066(1)	5.171(1)	7.552(2)	107.44(1)	107.96(1)	92.09(1)	177.72	7.106	7.370	7.780	88.83	119.23	91.18	355.45	(1)
$Cu_{67}Fe_{33}$	5.087(1)	5.170(1)	7.547(2)	107.16(1)	107.78(1)	92.35(1)	178.71	7.103	7.400	7.806	88.95	119.40	90.93	357.41	(1)
$Cu_{55}Fe_{45}$	5.115(1)	5.159(1)	7.540(2)	107.14(1)	107.48(1)	92.60(1)	179.38	7.098	7.428	7.819	89.44	119.51	90.49	358.77	(1)
$Cu_{46}Fe_{54}$	5.123(1)	5.159(1)	7.538(2)	107.04(1)	107.50(1)	92.76(1)	179.62	7.093	7.444	7.818	89.42	119.50	90.40	359.25	(1)
$Cu_{41}Fe_{59}$	5.131(1)	5.163(1)	7.546(2)	107.06(1)	107.42(1)	92.81(1)	180.28	7.098	7.455	7.829	89.52	119.50	90.36	360.56	(1)
$Cu_{34}Fe_{66}$	5.136(1)	5.163(1)	7.554(2)	107.07(1)	107.37(1)	92.93(1)	180.63	7.094	7.466	7.831	89.60	119.43	90.30	361.26	(1)
$Cu_{29}Fe_{71}$	5.148(1)	5.167(1)	7.564(2)	107.16(1)	107.40(1)	93.02(1)	181.24	7.099	7.483	7.827	89.70	119.34	90.21	362.49	(1)
$Cu_{25}Fe_{75}$	5.156(1)	5.161(1)	7.567(2)	107.26(1)	107.33(1)	93.06(1)	181.33	7.098	7.487	7.824	89.92	119.29	90.06	362.66	(1)
$Cu_{19}Fe_{81}$	5.163(1)	5.163(1)	7.576(2)	107.34(1)	107.35(1)	93.25(1)	181.64	7.092	7.506	7.813	89.99	119.13	90.00	363.28	(1)
Fe_{100}	5.177(1)	5.176(1)	7.608(2)	107.57(1)	107.57(1)	93.65(1)	182.58	7.084	7.550	7.779	90.01	118.63	89.99	365.16	(1)
Fe_{100}	5.174	5.174	7.600	107.55	107.55	93.69	182.24	7.078(3)	7.549(3)	7.773(3)	—	118.65(2)	—	364.48	(3)
Fe_{100}	5.160	5.160	7.624	107.55	107.55	92.71	182.41	7.123(9)	7.469(9)	7.837(9)	—	118.94(9)	—	364.82	(6)*
$Cu_{50}Fe_{50}$	5.120	5.120	7.480	106.71	106.71	92.94	177.96	7.053(9)	7.424(9)	7.853(9)	—	120.04(9)	—	355.92	(5)*
$Cu_{48}Fe_{52}$	5.120(1)	5.160(1)	7.535(2)	107.06(1)	107.40(1)	92.73(1)	179.59	7.094	7.440	7.824	89.47	119.56	90.45	359.18	(1)

Ref.: (1) this study, (2) Giester (1988), (3) Wildner & Giester (1991), (4) Coing-Boyat & Le Fur (1966), (5) Jambor (1962), (6) Pistorius (1960);
* original values are given in the reduced monoclinic setting $C2/c_R$

TABLE 3. D-I VALUES AND LEAST-SQUARES CELL PARAMETERS OF POITEVINITE (TRICLINIC INDEXATION)

a=5.124(3), b=5.163(3), c=7.535(5)Å, α=107.19(2), β=107.45(2), γ=92.75(2)°, FOM_{30}=27(0.023,49)

h k l	I/I_o	d_{cal}	d_{obs}	d_{dif}	*h k l*	I/I_o	d_{cal}	d_{obs}	d_{dif}	*h k l*	I/I_o	d_{cal}	d_{obs}	d_{dif}
0 1 0	29.0	4.8836	4.8504	.0332	2 -1 1	13.0	2.0848	2.0862	-.0013	0 3 -3	12.0	1.5872	1.5849	.0023
1 0 0	17.0	4.8326	4.7975	.0351	2 0 1	14.0	2.0732	2.0754	-.0022	3 0 -3	12.0	1.5798	1.5804	-.0006
-1 0 1	46.0	4.7394	4.7346	.0049	1 -2 2	11.0	2.0676	2.0677	-.0001	1 -1 -4	5.0	1.5508	1.5520	-.0012
1 0 -1	46.0	4.7394	4.7346	.0049	2 0 -3	5.0	2.0151	2.0158	-.0007	3 1 -3	9.0	1.5394	1.5388	.0006
1 -1 0	13.0	3.7217	3.7165	.0052	1 2 -3	6.0	1.9850	1.9866	-.0016	1 -2 -3	5.0	1.5134	1.5146	-.0013
1 1 -1	3.0	3.5448	3.5436	.0012	2 1 -3	23.0	1.9802	1.9787	.0014	1 -3 3	8.0	1.4715	1.4710	.0006
0 1 1	100.0	3.4722	3.4505	.0217	1 1 2	10.0	1.9525	1.9493	.0032	3 1 0	6.0	1.4665	1.4656	.0010
1 0 1	83.0	3.4439	3.4372	.0068	1 -1 3	5.0	1.9317	1.9333	-.0016	2 -3 1	6.0	1.4487	1.4483	.0004
1 0 -2	49.0	3.3443	3.3360	.0083	2 -2 0	7.0	1.8609	1.8623	-.0015	2 1 -5	11.0	1.4402	1.4395	.0006
0 1 -2	49.0	3.3431	3.3360	.0072	1 0 3	13.0	1.8353	1.8360	-.0007	0 1 -5	9.0	1.4363	1.4369	-.0006
1 -1 -1	30.0	3.2736	3.2681	.0054	1 -2 -2	5.0	1.7969	1.7964	.0005	3 1 -4	5.0	1.4227	1.4228	-.0001
1 -1 1	16.0	3.2570	3.2457	.0113	2 -1 2	5.0	1.7811	1.7805	.0006	2 3 -2	5.0	1.3945	1.3943	.0002
1 1 -2	79.0	3.0853	3.0738	.0115	1 2 1	4.0	1.7790	1.7787	.0003	3 -1 2	4.0	1.3404	1.3400	.0005
0 2 -1	9.0	2.5779	2.5856	-.0077	2 -1 -3	7.0	1.7641	1.7633	.0007	3 -1 -4	5.0	1.3198	1.3204	-.0006
2 0 -1	19.0	2.5559	2.5614	-.0056	1 -2 3	6.0	1.7596	1.7603	-.0007	0 4 -2	5.0	1.2890	1.2898	-.0008
1 -1 2	48.0	2.5037	2.5068	-.0031	2 0 2	6.0	1.7220	1.7228	-.0008	3 1 -5	9.0	1.2811	1.2820	-.0009
1 0 2	6.0	2.4325	2.4327	-.0002	0 3 -1	5.0	1.7132	1.7144	-.0012	1 -1 -5	9.0	1.2807	1.2804	.0003
2 0 0	8.0	2.4163	2.4185	-.0022	0 0 4	8.0	1.7012	1.7008	.0004	4 0 -2	8.0	1.2780	1.2782	-.0003
1 0 -3	9.0	2.3736	2.3722	.0014	0 3 -2	7.0	1.6970	1.6975	-.0005	1 -2 5	7.0	1.2593	1.2597	-.0004
0 1 -3	8.0	2.3700	2.3664	.0036	0 2 -4	27.0	1.6716	1.6709	.0007	1 1 -6	9.0	1.2511	1.2520	-.0009
1 -2 1	13.0	2.3058	2.3027	.0031	2 -2 -2	10.0	1.6368	1.6346	.0022	1 2 -6	4.0	1.2303	1.2301	.0002
2 -1 -1	13.0	2.2982	2.2969	.0013	2 -2 2	12.0	1.6285	1.6318	-.0034	2 0 4	5.0	1.2163	1.2165	-.0002
2 1 -1	21.0	2.2322	2.2299	.0023	1 -3 0	8.0	1.6168	1.6182	-.0014	3 3 -2	4.0	1.1735	1.1731	.0003
2 1 -2	3.0	2.2018	2.2040	-.0022	1 3 -2	11.0	1.6056	1.6074	-.0018	2 -4 2	7.0	1.1529	1.1528	.0001
1 -2 1	6.0	2.3058	2.1039	.2019	2 2 0	12.0	1.6029	1.6017	.0013					
0 2 1	13.0	2.0936	2.0955	-.0020	3 1 -2	15.0	1.5949	1.5949	.0000					

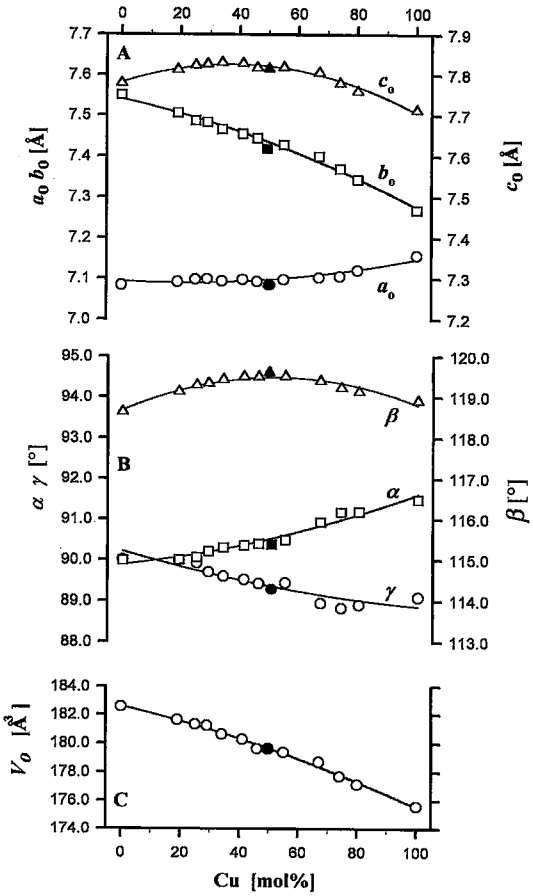

FIG. 3. Unit-cell parameters *a*, *b*, *c* (A), α, β, γ (B) for (Fe,Cu)SO_4·H_2O compounds in the monoclinic description (kieserite setting $C2/c_K$) and the triclinic cell volumes (C) for (Fe,Cu)SO_4·H_2O compounds. The filled symbols represent the respective values of poitevinite.

resented in terms of the kieserite setting (Figs. 3A, B). The *c* and β values show a parabolic trend with a slight maximum at 50% Fe, whereas the *a* and β values display a linear relationship over the whole solid-solution series, with negative and positive slope, respectively. The divergence from the "monoclinic" α and γ values (ideally 90°) represents the increasing triclinic distortion of the structure, with the monoclinic → triclinic transition occurring at ~ 80 mol.% Fe. The cell volume (Fig. 3C) shows a slight deviation from linearity that may result from preferential ordering of Fe and Cu within the structure. The cell parameters of poitevinite correspond closely to 50 mol.% Fe content as determined by ICP.

The *d* and I values of poitevinite based on triclinic indexing, together with the cell parameters and the figure of merit (Smith & Snyder 1979) of the least-squares refinement, are given in Table 3. The indexing and least-squares cell-parameter refinement of the *d* values were done with a PC-modified version of the algorithm of Appleman & Evans (1973).

Structure refinement: procedure

The initial atomic coordinates for the refinement in space group $P\bar{1}$ were taken from Giester (1988). The cation ratio Fe:Cu was not refined but fixed according to the results of the chemical analysis, and the isotropic displacement parameters of *M*1 and *M*2 were constrained to equal values. Although these restrictions were sufficient enough to obtain valid unit-cell parameters and indexing, the standard Rietveld refinement failed to provide reliable crystallochemical information about the $^{[6]}M$–O polyhedra. To improve the results of the refinement, restraints were applied to the SO_4 tetrahedra. The restraints (4 S–O and 6 O–O bond lengths) were allowed to vary within the range known from single-crystal analyses of the end members. To diminish the influence of texture, the region of the first four peaks was omitted in the refinement.

TABLE 4. EXPERIMENTAL CONDITIONS AND R-VALUES OF RIETVELD REFINEMENT

No. of observations	6500			
No. of parameters	32			
No. of restraints	2 S-O	1.49(4)		
	2 S-O	1.46(4)		
	6 O-O	2.41(3)		
No. of reflexions	1276(Cu) - 1332(Fe)			
	8 omitted			
	R_p	R_{wp}	R_e	R_B
Cu_{100}	11.5	14.0	3.2	6.5
$Cu_{80}Fe_{20}$	10.9	13.8	3.9	5.0
$Cu_{74}Fe_{26}$	12.7	16.3	4.0	4.2
$Cu_{67}Fe_{33}$	12.0	15.4	4.2	5.3
$Cu_{55}Fe_{45}$	11.1	15.0	4.0	6.5
$Cu_{46}Fe_{54}$	11.5	14.8	4.5	6.9
$Cu_{41}Fe_{59}$	11.0	14.0	4.1	6.4
$Cu_{34}Fe_{66}$	11.0	13.8	4.5	6.0
$Cu_{29}Fe_{71}$	11.8	15.1	4.6	7.1
$Cu_{25}Fe_{75}$	8.7	11.8	4.7	4.6
$Cu_{19}Fe_{81}$	8.0	10.4	4.8	4.5
Fe_{100}	7.5	9.4	5.8	4.9
$Cu_{48}Fe_{52}$	11.2	15.0	4.3	5.9

R_{wp}(%)	$\Sigma_i w_i(y_{oi}-1/C\cdot y_{ci})^2/\Sigma_i w_i y_{oi}^2)^{1/2}$
R_p(%)	$(\Sigma_i(y_{oi}-1/C\cdot y_{ci})/\Sigma_i y_{oi})$
R_e(%)	$((N-P)/\Sigma_i w_i y_{oi})^{1/2}$
R_B(%)	$\Sigma \mid I_{oi}-1/C\cdot I_{ci} \mid /\Sigma_i I_{oi}$
C	scale factor
y_o, y_c, y_b	observed, calculated and background profile intensities
I_o, I_c	observed and calculated integrated intensities
N	number of statistically independent observations
P	number of variable least-squares parameters
w	weight = $1/y_o$

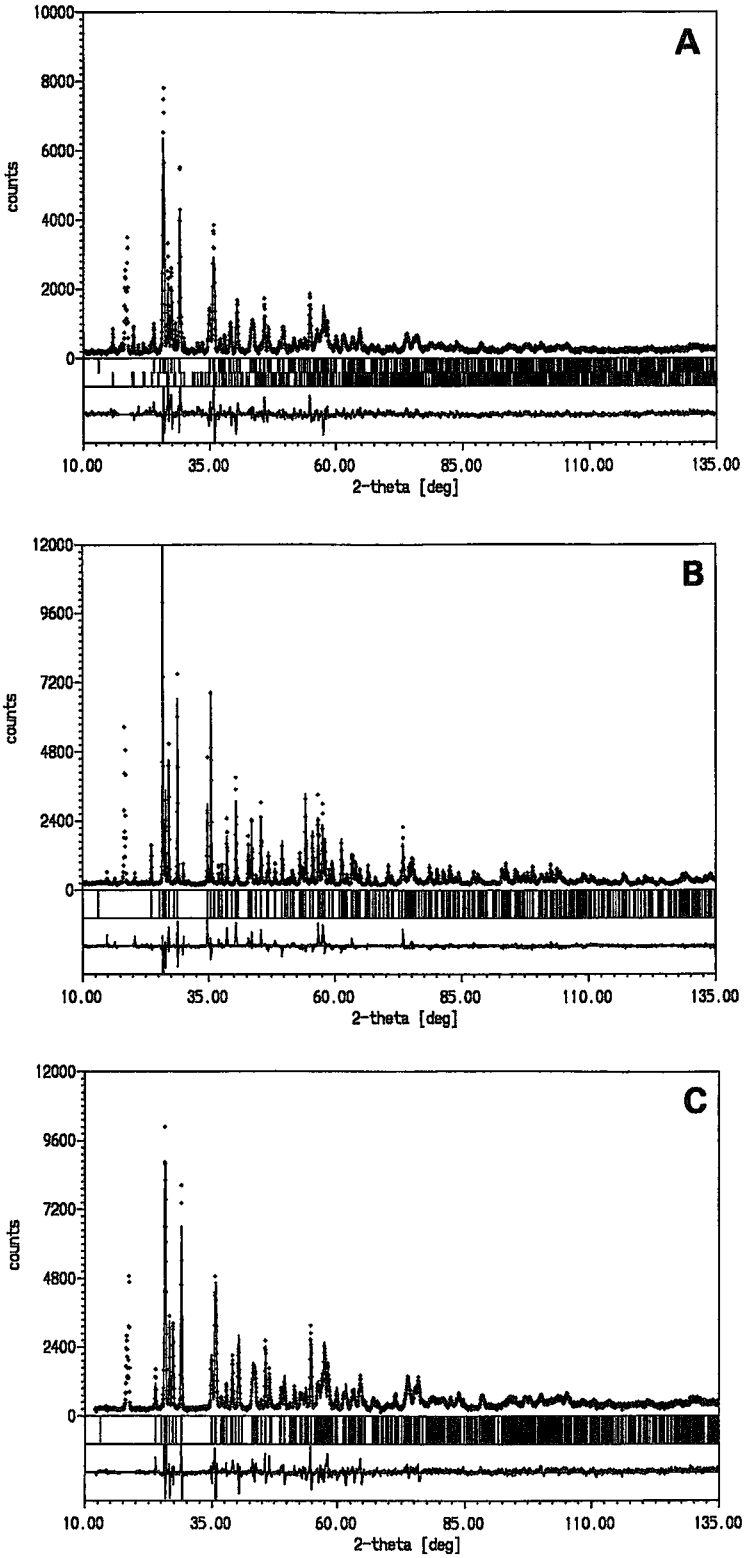

FIG. 4. Rietveld plots of poitevinite (A) and the end-member compounds $FeSO_4 \cdot H_2O$ (B) and $CuSO_4 \cdot H_2O$ (C). The lower tick marks in A represent the contribution of the scorodite impurity. The range 17–23° 2θ was omitted in the calculation.

Finally, the standard deviations of the structural parameters were corrected according to Bérar & Lelann (1991). The restraints and the final *R*-values are compiled in Table 4, and the Rietveld plots of poitevinite and the end members of the solid solution are given in Figure 4.

Mössbauer Spectroscopy

The Mössbauer spectra of synthetic (Fe,Cu) $SO_4 \cdot H_2O$ (Fig. 5) show two prominent lines centered at approximately –0.25 mm/s and 2.55 mm/s, equal in intensity and width, and giving Mössbauer parameters characteristic (Table 5) of high-spin $^{[6]}Fe^{2+}$. The FWHM of the absorption lines, determined by single-line fit over the range of the observed data, is between 0.29 and 0.31 mm/s. However, in pure $FeSO_4 \cdot H_2O$, the lines show a FWHM of only 0.23 mm/s, distinctly smaller than in the other samples. For this reason, the spectrum of synthetic szomolnokite was evaluated with only one doublet, whereas all other spectra were evaluated with a two-doublet fit. Our fit of two overlapping doublets to these spectra is justified because of the large FWHM and the significant decrease of the

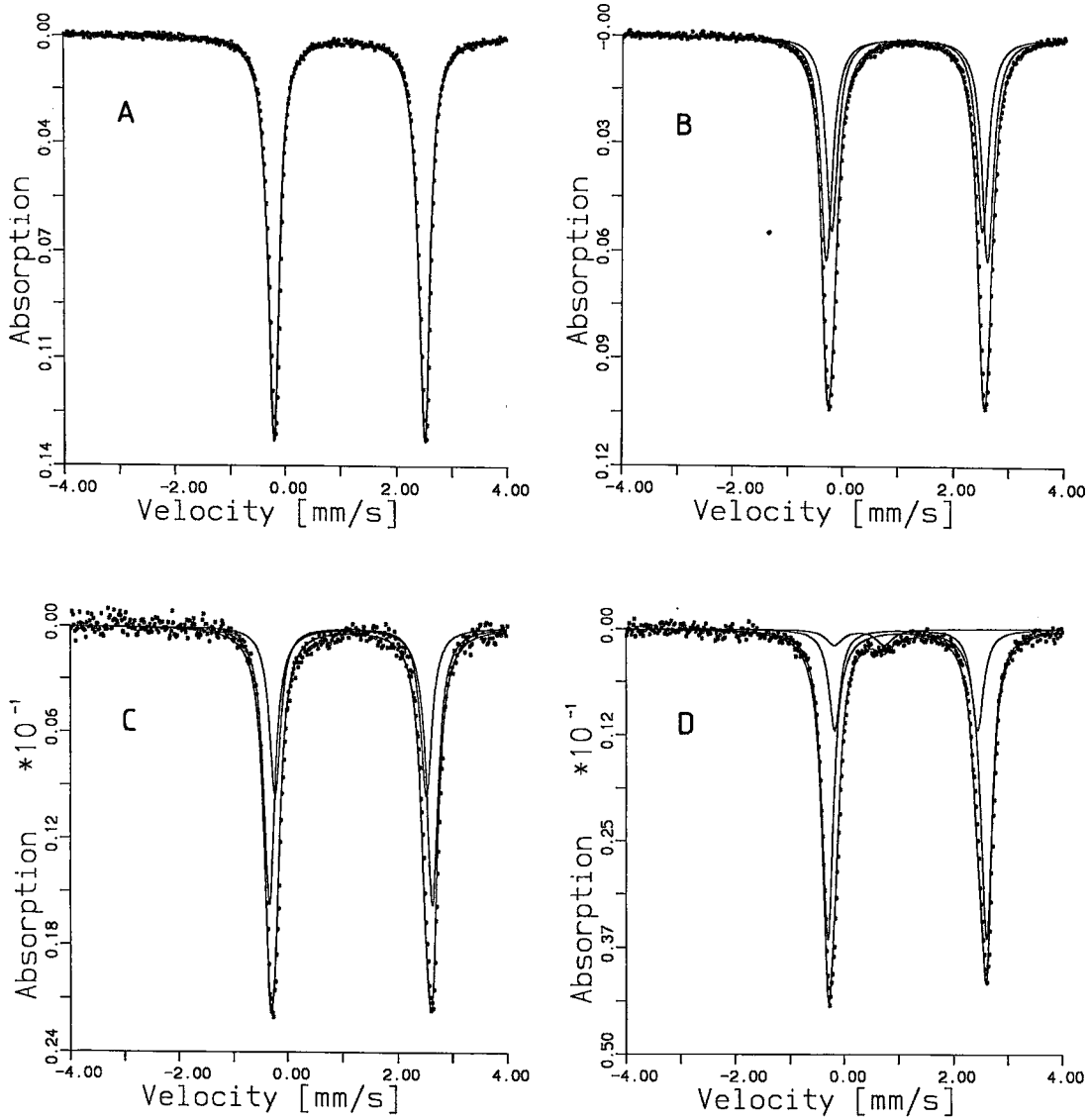

FIG. 5. Mössbauer spectra of Fe_{100} (A), $Fe_{45}Cu_{55}$ (B), $Fe_{26}Cu_{74}$ (C) and $Fe_{20}Cu_{80}$ (D) for (Fe,Cu)$SO_4 \cdot H_2O$ compounds.

TABLE 5. COMPILED MÖSSBAUER DATA

	IS(M1)	IS(M2)	QS(M1)	QS(M2)	A(M1)	A(M2)	FWHM
$Cu_{80}Fe_{20}$	1.24(1)	1.35(1)	2.60(1)	2.89(1)	24(1)	76(1)	0.24(1)
$Cu_{74}Fe_{26}$	1.25(1)	1.26(1)	2.70(1)	2.94(1)	23(1)	77(1)	0.23(1)
$Cu_{55}Fe_{45}$	1.25(1)	1.25(1)	2.72(1)	2.92(1)	32(1)	68(1)	0.23(1)
$Cu_{25}Fe_{75}$	1.25(1)	1.25(1)	2.71(1)	2.90(1)	46(1)	54(1)	0.23(1)
Fe_{100}	1.26(1)	—	2.71(1)	—	100	—	0.23(1)
$Cu_{48}Fe_{52}$	1.25(1)	1.25(1)	2.63(1)	3.03(1)	41(1)	59(1)	0.28(1)

IS: isomer shift [mm/s], QS: quadrupole splitting [mm/s], A: integrated area of the doublet [%], FWHM: full width of half maximum of both doublets [mm/s]

statistical parameter X^2. Furthermore, the basal tailing of the Lorentzian profiles showed major mismatch to the data-points with a one-doublet fit to the observed spectra. Two samples were measured at liquid-nitrogen temperature, but no improvement in resolution was observed. The area ratios do not change from room temperature to the temperature of liquid nitrogen.

The doublet with the lower quadrupole splitting (QS) was assigned to Fe^{2+} in the more distorted octahedron. The QS shows no significant variation with composition in the range from 100 to 50% $FeSO_4 \cdot H_2O$. Below this limit, the QS tends to decrease, indicating increasing distortion of the $M^{2+}O_6$ polyhedra.

The Mössbauer spectrum of poitevinite is similar to those of the synthetic phases. However, the differences in QS are more distinct. Besides the two ferrous doublets of poitevinite, one doublet attributed to Fe^{3+} occurs in the spectrum, and this can be assigned to the octahedrally coordinated iron of the scorodite impurity. The amount of scorodite in the poitevinite sample investigated is about 25 wt.%.

The area ratio of $Fe^{2+}(M2^{2+})/\Sigma Fe^{2+}$ obtained from the Mössbauer spectra shows a strong dependence on the Cu/Fe ratio of the samples. As the Cu content increases, Fe increasingly prefers the less distorted $M2^{2+}$ site, which implies that Cu is enriched at the $M1^{2+}$ position.

Discussion

Members of the solid-solution series $CuSO_4 \cdot H_2O$ – $FeSO_4 \cdot H_2O$ with a Cu content above 20 mol.% are triclinic-distorted. This could be a consequence of geometrical reasons only or could in addition reflect ordering of cations, as would be expected owing to the Jahn–Teller distortion of orbitals of divalent copper in

TABLE 6. ATOMIC COORDINATES, SELECTED DISTANCES AND ANGLES FOR POITEVINITE AND END-MEMBER COMPOUNDS, FROM RIETVELD REFINEMENT

		Fe_{100}	$Cu_{48}Fe_{52}$	Cu_{100}			Fe_{100}	$Cu_{48}Fe_{52}$	Cu_{100}
M1			0,0,0		M2			1/2,1/2,1/2	
	B[1]	0.9(5)	1.1(6)	0.7(5)		B	0.9(5)	1.1(6)	0.7(5)
S	x	0.596(2)	0.593(2)	0.608(3)	$O(H_2O)$	x	0.103(6)	0.114(6)	0.125(6)
	y	0.899(2)	0.918(2)	0.925(3)		y	0.392(7)	0.407(7)	0.430(6)
	z	0.248(2)	0.248(2)	0.243(3)		z	0.255(6)	0.265(6)	0.284(5)
	B	0.8(6)	0.7(6)	0.4(7)		B	1.4(7)	1.0(8)	1.6(9)
O1	x	0.724(6)	0.727(6)	0.752(6)	O2	x	0.291(6)	0.287(6)	0.301(6)
	y	0.815(5)	0.830(5)	0.829(6)		y	0.827(6)	0.828(6)	0.836(6)
	z	0.097(5)	0.098(5)	0.095(4)		z	0.154(5)	0.154(5)	0.142(5)
	B	1.9(5)	1.1(6)	1.3(7)		B	1.1(8)	1.3(7)	1.9(8)
O3	x	0.668(6)	0.644(6)	0.663(6)	O4	x	0.689(6)	0.694(6)	0.707(6)
	y	0.204(6)	0.222(6)	0.232(5)		y	0.765(6)	0.797(6)	0.808(6)
	z	0.345(5)	0.331(5)	0.322(5)		z	0.394(5)	0.404(5)	0.399(5)
	B	2.0(6)	0.9(7)	1.5(7)		B	1.4(5)	1.6(5)	1.1(7)
M1-O1		2.10(2)	2.04(2)	1.95(2)	O1-M1-O2		86.2(8)	86.7(9)	86.8(9)
M2-O4		2.11(2)	2.19(2)	2.33(2)	O4-M2-O3		84.8(8)	86.3(9)	81.6(8)
M1-O2		2.05(2)	2.00(2)	1.94(2)	O1-M1-O(H_2O)		87.2(9)	86.9(10)	85.8(9)
M2-O3		2.05(2)	1.95(3)	1.99(2)	O4-M2-O(H_2O)		85.4(10)	84.4(10)	84.9(9)
M1-O(H_2O)		2.24(4)	2.34(4)	2.45(3)	O2-M1-O(H_2O)		87.9(10)	88.9(10)	89.0(10)
M2-O(H_2O)		2.22(3)	2.14(3)	2.01(3)	O3-M2-O(H_2O)		87.4(11)	88.9(11)	88.0(10)
					M1-O(H_2O)-M2		121.4(8)	121.6(9)	119.6(8)

[1]Isotropic displacement parameters of the M1 and M2 position are constrained to equal values, atomic coordinates and displacement parameters of all other compounds are deposited at the Canadian Institute for Scientific and Technical Information

octahedral coordination.

Considering anomalous dispersion (Cu$K\alpha$), the scattering factors of Cu and Fe differ only by half an electron in the low-angle region, preventing the refinement of the cation distribution over the $M1^{2+}$ and $M2^{2+}$ sites. The intensity of the (001) reflection, which is forbidden in *C*2/*c*, cannot be observed ($I/I_0 < 0.1\%$). In the analogous (Cu,Mg)$SO_4 \cdot H_2O$ series (Lengauer & Giester 1995), however, the larger differences of the scattering factors allow the observation of the (001) reflection and the refinement of the Cu/Mg ratio on the respective $M1^{2+}$ (predominantly Cu) and $M2^{2+}$ (predominantly Mg) sites, implying that an analogous ordering could occur in the (Cu,Fe)$SO_4 \cdot H_2O$ samples.

The Mössbauer spectra indicate ordering of Fe^{2+} at the more regular $M2^{2+}$ site. Besides, the nonlinear trends in the variation of some cell parameters and of the cell volume agree with the results of the Mössbauer spectroscopy.

Annealing the rapidly precipitated compounds of the series (method 1) not only led to an improvement of crystallinity, *i.e.*, sharpening of the diffraction maxima, but also to an increase of the departure from monoclinic symmetry. As the chemical composition of the samples is not affected by this procedure, the change in the cell parameters is presumably due to increased degree of order.

The Rietveld refinement of end members of the solid solution with the restraints of the SO_4 tetrahedra-led to mean $^{[6]}M$–O values for divalent copper and ferrous iron in octahedral coordination that compare well with single-crystal data (Giester 1988, Wildner & Giester 1991) within the standard deviation of the Rietveld refinement (Table 6). The main difference between Cu and Fe is the pronounced [4+2] elongation of the Jahn–Teller-distorted CuO_6 polyhedron. This is also evident in the results of the Rietveld refinements: with increasing Cu content, the *M* positions become more distorted (Fig. 6); the *M*1 position is the more elongate one.

The *M*1 polyhedra show a steadily increasing distortion with increasing Cu content of the compounds. The *M*1–O1 and *M*1–O2 distances decrease slightly from 2.10(2), 2.05(2) to 1.95(2), 1.94(2) Å, respectively. The *M*1–O(H_2O) distance, however, increases from 2.24(4) to 2.45(3) Å. The degree of distortion of the *M*2 polyhedra is less affected by chemistry for Cu contents less than 50%. At higher Cu contents, an increasing distortion is also evident for *M*2. The *M*2–O3 bond length decreases from 2.05(2) to 1.99(2) Å, whereas the distances of *M*2–O4 [2.11(2) to 2.33(2)] and the *M*2–O(H_2O) [2.22(3) to 2.01(3)] show a different trend with respect to the *M*1 polyhedra. The results for poitevinite, compiled in Table 6, are in a good agreement to the values of the analogous synthetic compound. Note that atomic coordinates and displacement parameters of all other compounds synthesized in this investigation are available from The

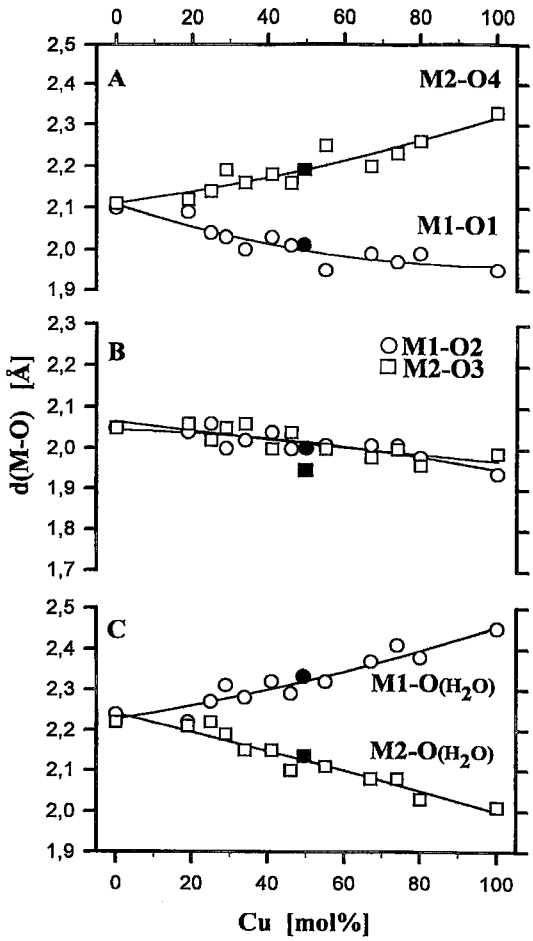

FIG. 6. Distances of the $^{[6]}M$–O polyhedra for (Fe,Cu)$SO_4 \cdot H_2O$ compounds. The filled symbols represent the respective values of poitevinite.

Depository of Unpublished Data, CISTI, National Research Council of Canada, Ottawa, Ontario K1A 0S2.

In the Mg–Cu solid-solution series, the compounds with an approximately equimolar Mg:Cu ratio were found to precipitate most easily and to be better crystallized (Lengauer & Giester 1995). Analogous properties may be attributed to the poitevinite series; the thermal stability, for example, is about 100 K higher for the intermediate representatives than for the end members.

A remarkable feature of poitevinite is its intense reddish orange color, which does not fade down to a temperature of 90 K. There is no indication that minor amounts of ferric iron are preferentially incorporated

in the intermediate compounds, thus making a Fe^{2+}/Fe^{3+} charge transfer unlikely to cause the color. Optical spectra would be a promising way to study the origin of the color, but so far no suitable crystals of poitevinite are available.

In conclusion, with respect to degree of cation order and triclinic distortion of the unit cell, we can confirm that poitevinite (triclinic) is an independent mineral, considering the guidelines of mineral nomenclature in solid-solution series (Nickel 1992).

Acknowledgements

The authors are grateful to R.I. Gait from the Royal Ontario Museum for supplying the type material of poitevinite, to Eugen Libowitzky, Peter Unfried and Monika Leodolter for their assistance with the chemical analyses, to Ekkehart Tillmanns and Josef Zemann for valuable comments, and to the anonymous referees for critically reading the manuscript. Special thanks to Karl Forcher and Werner Lottermoser for their assistance with the Mössbauer measurements.

References

Appleman, D.E. & Evans, H.T., Jr. (1973): Indexing and least-squares refinement of powder diffraction data. *U.S. Geol. Surv., Comput. Contrib.* **20**, *U.S. Nat. Tech. Information Service, Doc.* **PB2-16188**.

Baur, W.H. (1959): Über kristallstrukturelle Beziehungen zwischen Amblygonit, Kieserit und Titanit. *Beitr. Mineral. Petrogr.* **6**, 399-404.

Bérar, J.-F. & Lelann, P. (1991): E.S.D.'s and estimated probable errors obtained in Rietveld refinements with local correlations. *J. Appl. Crystallogr.* **24**, 1-5.

Bohm, M. (1992): CRYSCOMP, Version 1992. Berlin, Germany (unpubl.).

Bowden, M.E. & Ryan, M.J. (1991): Comparison of intensities from fixed and variable divergence X-ray diffraction experiments. *Powder Diffraction* **6**, 78-84.

Caglioti, G., Paoletti, A. & Ricci, F.P. (1958): Choice of collimators for a crystal spectrometer for neutron diffraction. *Nucl. Instr.* **3**, 223-228.

Coing-Boyat, J. & Le Fur, Y. (1966): Maille triclinique du sulfate de cuivre-II monohydraté. *C.R. Acad. Sci. Paris* **262**, *Sér.* **B**, 722-725.

Dowty, E. (1993): ATOMS (version 2.3) – a computer program for displaying atomic structures. Kingsport, Tennessee.

Fischer, R.X. (1993): Divergence slit corrections for Bragg Brentano diffractometers. *Third European Powder Diffraction Conf., Abstr.*, 25.

———, Lengauer, C.L., Tillmanns, E., Ensink, R.J., Reiss, C.A. & Fantner, E.J. (1993): PC-Rietveld plus, a comprehensive Rietveld analysis package for PC. *Materials Science Forum* **133-136**, 287-292.

Forcher, K., Kaliba, F. & Lottermoser, W. (1992): MOESALZ – a computer program for Mössbauer data evaluation. Universität Salzburg, Salzburg, Austria.

Giester, G. (1988): The crystal structures of $CuSO_4 \cdot H_2O$ and $CuSeO_4 \cdot H_2O$, and their relationship to kieserite. *Mineral. Petrol.* **38**, 277-284.

——— & Wildner, M. (1992): The crystal structures of kieserite-type compounds. II. Crystal structures of $Me(II)SeO_4 \cdot H_2O$ (Me = Mg,Mn,Co,Ni,Zn). *Neues Jahrb. Mineral., Monatsh.*, 135-144.

Groat, L.A., Raudsepp, M., Hawthorne, F.C., Ercit, T.S., Sherriff, B.L. & Hartman, J.S. (1990): The amblygonite – montebrasite series: characterization by single-crystal structure refinement, infrared spectroscopy, and multinuclear MAS–NMR spectroscopy. *Am. Mineral.* **75**, 992-1008.

Hawthorne, F.C., Groat, L.A., Raudsepp, M. & Ercit, T.S. (1987): Kieserite, $Mg(SO_4)(H_2O)$, a titanite-group mineral. *Neues Jahrb. Mineral., Abh.* **157**, 121-132.

Hovestreydt, E. (1983): On the atomic scattering factor of O^{2-}. *Acta Crystallogr.* **A39**, 268-269.

International Tables for X-Ray Crystallography, Vol. IV (1974): Revised and Supplementary Tables (J.A. Ibers & W.C. Hamilton, eds.). The Kynoch Press, Birmingham, U.K.

Isaacs, A.M. & Peacor, D.R. (1981): Panasqueiraite, a new mineral: the OH-equivalent of isokite. *Can. Mineral.* **19**, 389-392.

Jambor, J.L. (1962): Second occurrence of bonattite. *Can. Mineral.* **7**, 245-252.

———, Lachance, G.R. & Courvilles, S. (1964): Poitevinite, a new mineral. *Can. Mineral.* **8**, 109-110.

Kassner, D. (1993): RERIET, PC-version 1993. Frankfurt, Germany (unpubl.).

Lahti, S.I. & Pajunen, A. (1985): New data on lacroixite, $NaAlFPO_4$. *Am. Mineral.* **70**, 849-855.

Leonhardt, J. & Weiss, R. (1957): Das Kristallgitter des Kieserits $MgSO_4 \cdot H_2O$. *Naturwiss.* **44**, 338-339.

Lengauer, C.L. & Giester, G. (1995): Rietveld refinement of the solid-solution series: $(Cu,Mg)SO_4 \cdot H_2O$. *Powder Diffraction* (in press).

Nickel, E.H. (1992): Solid solutions in mineral nomenclature. *Can. Mineral.* **30**, 231-234.

OSWALD, H.R. (1965): Über die Bindung der Wassermolekel in den Verbindungen $Me^{II}SO_4,1H_2O$ und $Me^{II}SeO_4,1H_2O$. I. Strukturuntersuchungen. II. Infrarotspektrographische und kernmagnetische Resonanz-Untersuchungen (Me^{II} = Mg,Ni,Cu,Co,Fe,Zn,Mn). *Helv. Chim. Acta* **48**, 590-608.

PISTORIUS, C.W.F.T. (1960): Lattice constants of $FeSO_4{\cdot}H_2O$ (artificial szomolnokite) and $NiSO_4{\cdot}H_2O$. *Bull. Soc. Chim. Belg.* **69**, 570-574.

RIETVELD, H.M. (1969): A profile refinement for nuclear and magnetic structures. *J. Appl. Crystallogr.* **2**, 65-71.

SMITH, G.S. & SNYDER, R.J. (1979): F_N: a criterion for rating powder diffraction patterns and evaluating the reliability of powder-pattern indexing. *J. Appl. Crystallogr.* **12**, 60-65.

WILDNER, M. & GIESTER, G. (1991): The crystal structures of kieserite-type compounds. I. Crystal structures of $Me(II)SO_4{\cdot}H_2O$ (Me = Mn,Fe,Co,Ni,Zn). *Neues Jahrb. Mineral., Monatsh.*, 296-306.

ZEMANN, J. (1990): Die Strukturtypen des Lazuliths, Lipscombits, Caminits und Kieserits: eine Gruppe topologisch eng verwandter Atomanordnungen. *Aufschluss* **41**, 7-11.

Received August 31, 1993, revised manuscript accepted January 27, 1994.